AD-A082 392 MOORE SCHOOL OF ELECTRICAL ENGINEERING PHILADELPHIA PA F/G 9/3
HIGH RESOLUTION FREQUENCY SWEPT IMAGING.(U)
FEB 80 N H FARHAT DAAG29-76-G-0230
UNCLASSIFIED ARO-13366.12-EL NL

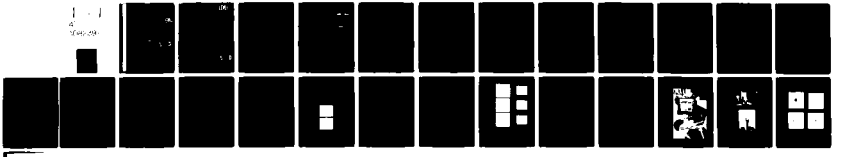

END
DATE FILMED
4 80
DTIC

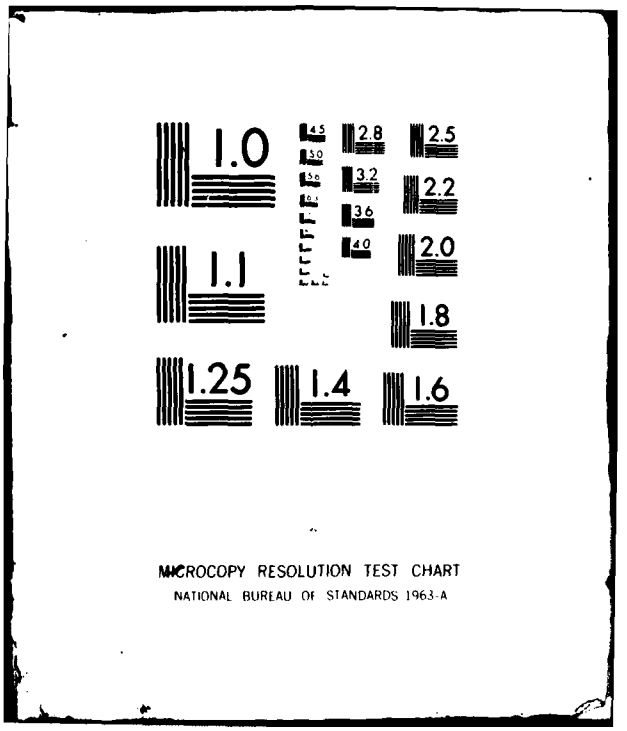
1.0
1.1
1.25
1.4
1.6
1.8
2.0
2.2
2.5
2.8
3.2
3.6
4.0
4.5
5.0
MICROCOPY RESOLUTION TEST CHART
NATIONAL BUREAU OF STANDARDS 1963-A

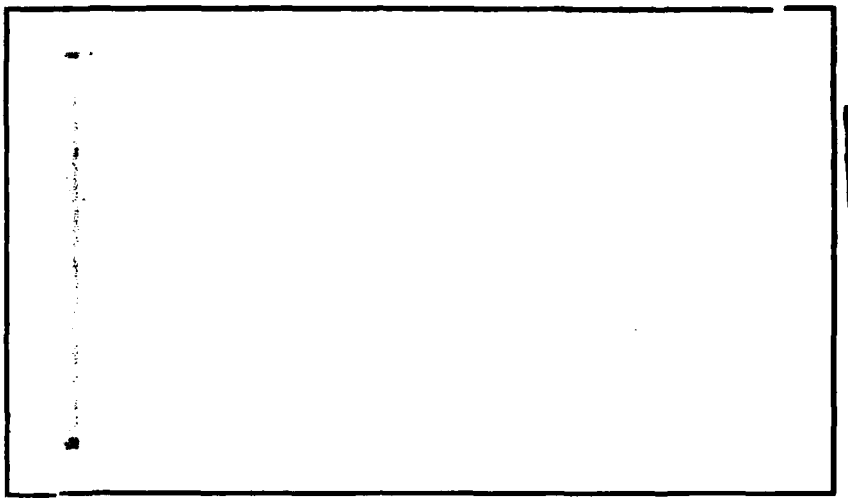

UNIVERSITY of PENNSYLVANIA

The Moore School of Electrical Engineering

PHILADELPHIA, PENNSYLVANIA 19104

(12) LEVEL II

HIGH RESOLUTION FREQUENCY SWEPT IMAGING

FINAL REPORT

PREPARED BY :
N.H. FARHAT

FEBRUARY 14, 1980

U.S. ARMY RESEARCH OFFICE

GRANT NUMBER: DAAG29-76-G-0230

UNIVERSITY OF PENNSYLVANIA
THE MOORE SCHOOL OF ELECTRICAL ENGINEERING
PHILADELPHIA, PENNSYLVANIA

The findings in this report are not to be construed as an official department of the Army position, unless so designated by other authorized documents.

SECURITY CLASSIFICATION OF THIS PAGE (When Data Entered)

REPORT DOCUMENTATION PAGE

READ INSTRUCTIONS BEFORE COMPLETING FORM

1. REPORT NUMBER: 21
2. GOVT ACCESSION NO.
3. RECIPIENT'S CATALOG NUMBER
4. TITLE (and Subtitle): High Resolution Frequency Swept Imaging.
5. TYPE OF REPORT & PERIOD COVERED: Final report, 15 Jun 76-Dec 80
6. PERFORMING ORG. REPORT NUMBER: 14
7. AUTHOR(s): N.H. Farhat
8. CONTRACT OR GRANT NUMBER(s): DAAG29-76-G-0230
9. PERFORMING ORGANIZATION NAME AND ADDRESS:
University of Pennsylvania
The Moore School of Electrical Engineering
200 S. 33rd St. Phila., PA 19104
10. PROGRAM ELEMENT, PROJECT, TASK AREA & WORK UNIT NUMBERS
11. CONTROLLING OFFICE NAME AND ADDRESS:
U.S. Army Research Office
Post Office Box 12211
Research Triangle Park, NC 27709
12. REPORT DATE: 14 Feb 80
13. NUMBER OF PAGES: 25
14. MONITORING AGENCY NAME & ADDRESS (if different from Controlling Office)
15. SECURITY CLASS. (of this report): unclassified
15a. DECLASSIFICATION/DOWNGRADING SCHEDULE: N/A
16. DISTRIBUTION STATEMENT (of this Report):

Approved for public release; distribution unlimited.

18 ARO 19 13366.12-EL

17. DISTRIBUTION STATEMENT (of the abstract entered in Block 20, if different from Report)

N/A

18. SUPPLEMENTARY NOTES

The findings in this report are not to be construed as an official Department of the Army position, unless so designated by other authorized documents.

19. KEY WORDS (Continue on reverse side if necessary and identify by block number)

Longwave imaging, frequency diversity, super-resolution, Fourier domain projection, tomographic displays, cost-effective apertures.

20. ABSTRACT (Continue on reverse side if necessary and identify by block number)

High resolution (microwave or ultrasound) apertures suitable for use in single frequency longrange imaging radar (or sonar) are prohibitively expensive and difficult, if not impossible, to implement. In addition they are expected to suffer from image degration by speckle or coherent noise that is a drawback of all monochromatic imaging systems. Also their longitudinal resolution is expected to deteriorate rapidly with range.

DD FORM 1 JAN 73 1473 EDITION OF 1 NOV 65 IS OBSOLETE

237000 DW

SECURITY CLASSIFICATION OF THIS PAGE (When Data Entered)

20.Abstract - continued

The effort described in this final report has been initiated to study frequency or wavelength diversity techniques as a means of overcoming some or all of the above limitation. A primarily analytical and numerical study of frequency diversity imaging has lead to the following major findings:

Such broadband techniques can be employed to enhance the information content of the wavefield scattered by a coherently illuminated object and collected by a recording aperture through a process of aperture synthesis by frequency diversity (swept, stepped or multifrequency illumination and detection).

We have been able to find procedures by which frequency diversity data collected by a broadband highly thinned and therefore cost-effective aperture can be made to yield a super-resolved 3-D image of a distant scatterer. These procedures rely on:(a) the use of a *target derived reference (TDR)* technique which provides a more direct accessing of the 3-D Fourier space of the scattering object, (b) the use of hybrid (digital/optical) processing based on *Fourier domain projection theorems* to retrieve and display 3-D image detail *tomographically* in parallel or meridonal slices or cross-sectional outlines one at a time. Views of a true 3-D image of the scattering object appears also to be possible by display of adjacent cross-sectional outlines one after the other in rapid succession in arrangements that make use of a rapid recyclable spatial light modulator and instantaneous 2-D optical Fourier transformation.

The findings of this research effort provide basic principles and procedures for a new generation of *super-revolving, cost-effective, tomographic* imaging radars (or sonars) capable of converting spectral degrees of freedom in the wavefields coherently mapped by their broad-band apertures into 3-D image detail.

Computer simulations suggest that giant highly thinned apertures formed by a small number of broadband receiving stations that can be as low as ten stations all of which employing a TDR used in conjunction with a single central illuminator can be made to yield 10^3 3-D resolution cells in object space by using merely 100 frequency points in a (2-4) GHz sweep range.

Experimental verification of the basic concept of frequency diversity imaging was obtained with the aid of an available semi-automated microwave network analyzer for a test object situated in an anechoic chamber.

TABLE OF CONTENTS

HIGH RESOLUTION FREQUENCY SWEPT IMAGING

1. Introduction

The aim of the research work outlined in this final report was the analysis and investigation of methods by which frequency or wavelength diversity techniques can be employed to impart to a highly thinned, and therefore cost-effective, longwave (microwave or ultrasound) imaging aperture resolution capabilities better than its monochromatic classical (Rayligh) limit achieving thereby super-resolution by means of frequency synthesized apertures. This approach to longwave imaging gains practical significance when one considers the current highly developed state of the art of broadband microwave gear suitable for use in a new generation of cost-effective high resolution microwave imaging radars utilizing frequency diversity techniques.

It is well known that the development of longwave holographic imaging systems possessing resolution and image quality approaching those of optical systems is hampered by three factors: (a) prohibitive cost and size of longwave imaging apertures, (b) rapid deterioration of longitudinal resolution with range, (c) inability to view a 3-D image as with optical Fresnel holograms because of a wavelength scaling problem and (d) degradion of image quality by speckle or coherent noise because of the low numerical apertures attainable with present techniques. For example, a longwave imaging aperture operating at a wavelength of 3 cm should be about 3 km in size in order to achieve image resolution comparable to an ordinary photographic camera. In addition to inconvenient size, the cost of filling such a large aperture with suitable coherent sensors is clearly prohibitive. Furthermore, recall that in conventional longwave holography when optical image retrieval is utilized, it is necessary to store the longwave hologram data (fringe pattern) in an optical transparency suitable for processing on the optical bench using laser light. In order to avoid longitudinal distortion* of the reconstructed image, the size of the optical hologram replica must be m ($=\lambda_{long}/\lambda_{laser}$) times smaller than the longwave recording aperture. For the example cited earlier, this means an optical hologram replica of less than a millimeter in size. It is certainly not possible to view a virtual 3-D image through such a minute hologram even with optical aids since these tend to introduce their own longitudinal distortion. As a result, longwave holographers have long learned to forgo 3-D imagery and settled instead for 2-D imagery obtained by projecting the reconstructed real image on a screen. This permits lowering of the reduction factor m and consequently relaxing the resolution requirements of the photographic film which allows in turn the use of highly convenient Polaroid transparency film for preparation of the optical hologram replica. Because of the small size (measured in wavelength) of longwave apertures attainable in practice and the above methods of viewing the real image, speckle noise is always present leading to degration in image quality.

* Longitudinal distortion causes for example the image of a sphere to appear elongated in the range direction like a very long ellipsoid.

In this report we summarize the main results of our investigation under this grant. Our findings show that frequency diversity techniques not only circumvent the limitations discussed above but provide a means of viewing true 3-D images of distant objects such as satellites and aircraft. It is worthwhile to point out that our studies of wave-vector diversity imaging (or frequency swept imaging) were motivated to some extent by evidence of super-resolved "imaging" capabilities in the dolphin and the bat which are known to use frequency swept (chirp) signals in their "sonar" to discern small objects in their environment.

2. Summary of Important Results

The main findings of the study, details of which are given in our publications (see list of publications), are outlined next.

(a) Wave-vector diversity (multifrequency and multiaspect) techniques can be used to enhance the amount of object information collected by a broadband coherent aperture deployed in the far field of the scattering object. Thus the data collected by a highly thinned array of coherent receivers intercepting the wavefield scattered from a distant 3-D reflecting object, as the frequency of its illumination (and/or its direction of incidence) are changed (see Fig. 1-a for example), can be stored as a 3-D data manifold in $\bar{p}$-space (Fig. 2) from which an image of the object can be retrieved by means of a 3-D Fourier Transform. The size and shape of the 3-D data manifold, and therefore the resolution, depend on the relative positions of the object, the transmitter (illuminator), and the receiving array and on the spectral width of the illumination utilized.

(b) The data collected must be corrected for a quadratic phase factor F (caused by the unequal distances between the object and the receiving stations forming the widely dispersed imaging array) before it is stored in a 3-D manifold in $\bar{p}$-space and an undistorted image of the 3-D reflecting object reconstructed through the 3-D Fourier transform operation. A bothersome range-azimuth ambiguity is also avoided through elimination of this quadratic phase term.

The most promising methods for data acquisition and correction is that which utilizes a target derived reference (TDR) at the synchronous detectors of the various receivers to correct for the unequal phase shifts or propagation time delays from the object to each receiver. In this approach the data furnished by the various receivers of the recording array is free of the undesired factor F. Therefore no additional processing by a computer will be necessary before filing the data at the appropriate locations in $\bar{p}$-space. The TDR method has several advantages which include:

(i) Elimination of the need for a costly and unreliable central local oscillator distribution network.

(ii) Because TDR results in a recording configuration similar to that of a lensless Fourier Transform hologram, the resolution requirements from the recording device are greatly relaxed*.

*A. Macovski, "Hologram Information Capacity", J. Opt. Soc. Am., Vol. 60, Jan. 1970, pp. 21-29.

In longwave holography this fact is translated into a significant reduction of the number of receiving elements in the recording aperture. In addition the use of TDR allows us to place all the resolving power of the recording aperture on the target. This means that high resolution images of distant isolated targets should be feasible with array apertures consisting of tens of elements. The ability to synthesize a 2-D receiving aperture with a Wells array† consisting of two orthogonal linear arrays one of transmitters and the other of receivers provides further means of reducing the number of stations needed for data acquisition without sacrifice in resolution. A frequency swept Wells array of 10 transmitters and 10 receivers using a (2-4) GHz sweep should be able to easily furnish 10^4 3-D distinguishable resolution cells on the target which is more than sufficient for discerning the scattering centers on practical targets.

(iv) Greater immunity to phase fluctuations arising from turbulance and inhomogenieties in the propagation medium because both the reference and imaging signals arriving at each receiving element of the aperture travel roughly over the same path.

(v) TDR eliminates the range azimuth ambiguity and excessive bandwidth problems that arise in fast frequency swept imaging when the reference signal for the array aperture is distributed instead from the illumination source or a centrally located local oscillator phase locked to it.

Two TDR methods have been considered to some extent in our work to date. In one method which we term LFTDR (*Low Frequency Target Derived Reference*), the object is assumed to be illuminated simultaneously with a high frequency imaging signal and a low frequency signal that is a subharmonic of the illuminating frequency. The subharmonic reference frequency ω_r is chosen such that $k_r \ell << 1$, ℓ being the maximum linear dimension of the object and $k_r = \omega_r/c$, c being the velocity of light. This places scattering from the object in the Rayliegh region where the object behaves as point scatterer with zero phase contribution. The far field phase of the reference signal at any receiver is therefore entirely due to propagation between a reference point formed at the object to the receiver. A method for measuring this reference signal phase and using it to correct the imaging signal phase due to propagation has been proposed by Porter* and analyzed for a one-dimensional object geometry. The reference signal phase and the imaging signal phase are measured separately at each receiving station with the aid of two receivers whose local oscillators (L.O)'s, one at the reference frequency and one at the imaging frequency, are phase-locked only to each other and not to a central local oscillator as would be the case were we to use a conventional receiver array. Phase locking of the two LO's can be accomplished by simply making the imaging L.O a harmonic of the

†C.N. Nilsen and D.N. Swingler, "Quasi-Real-Time Inertialess Microwave Holography", Proc. IEEE (Letters), Vol. 65, March 1975, pp. 491-492.
*R.P. Porter, "A Radar Imaging System Using the Object as Reference", Proc. IEEE (Letters), Vol. 59, Feb. 1971, pp. 307-308.

reference L.O. This would eliminate the difficulties encountered in the implementation of large or giant thinned coherent receiving arrays of the type required here, namely the distribution of a central local oscillator signal. A great reduction in cost and effort associated with installation of a central L.O. distribution network can thus be achieved. This cost reduction should be compared however with the cost of implementing a LFTDR. Because of the large difference between the high frequency imaging frequencies and the low frequency reference frequency required for the high resolution imaging of practical objects, the same microwave gear can not be used for both frequencies. This could increase system cost. In addition since the measured reference phase must be multiplied by a factor β equal to the ratio of the imaging to the reference frequency before being used as a reference phase in the imaging signal measurement, any errors in the reference phase measurement will also be amplified by this ratio. The precision of the reference phase measurement and phase error analysis are important and will have therefore to be considered.

Another TDR methods which we call the *Frequency Displaced Target Derived Reference* (FDTDR) also shows promise. In this method, the analytical details of which are outlined in appendix I, the object is illuminated simultaneously during the sweep with two phase locked imaging frequencies ω_1 and $\omega_2 = \omega_1 + \Delta\omega$, $\Delta\omega$ being a small incremental frequency. This can be realized also by single side band modulation of the swept signal or by phase locking two sweep oscillators. Measurement of the differential phase between the signals scattered from the target at these frequencies yields $\frac{\Delta\omega}{c}(R_T + R_R)$, R_T being the distance from the transmitter to the object and R_R being the distance from the object to the receiver. Multiplication of this phase by $\omega_1/\Delta\omega$ yields the phase factor F at frequency ω_1 which would be used to correct the phase measured at ω_1. At first look this method would appear to still require a reference local oscillator. This however is not so since the procedure outlined above need not involve explicit phase measurements and multiplications. For example by mixing the two received signals at ω_1 and $\omega_1 + \Delta\omega$ in a square law detector at each receiver a beat signal at frequency $\Delta\omega$ is derived whose phase is equal to $\frac{\Delta\omega}{c}(R_R + R_T)$. The phase shift of this signal due to the object is effectively zero because the wavelength at $\Delta\omega$ is much larger than the object extent making it behave effectively as a point scatterer. Harmonic mixing of the signal ω_1 received at each receiver with this beat signal should yield the corrected p-space data at ω_1. Because of the small difference $\Delta\omega$ between the two frequencies ω_1 and ω_2 utilized, the effect of phase errors due to system and atmospheric propagation could be more completely cancelled in this method than in the low frequency TDR methods. The small difference $\Delta\omega$ means also that unlike the LFTDR case the same microwave gear (antennas, transmission lines and other microwave circuit components) can be utilized in the handling of the reference and imaging signals. A variation of the TDR technique involving double side-band modulation is also possible and appears to be more simple to implement than the single side-band method.

(c) Because in addition to being dependent on geometry, the dimensions of the 3-D data in $\bar{p}$-space shown in Fig. 2 are dependent on the spectral range of the illumination, super-resolution (i.e. resolution beyond the classical limit of the available physical aperture) is achieved. This aperture synthesis by wave-vector or frequency diversity helps cut down array cost (since a thinned array can be used to frequency synthesize a large array with higher filling factor).

(d) *Fourier Domain Projection Theorems* (see Ref. 10 in List of publications) enable the generation of two dimensional holograms from projections (or weighted projections) of the corrected $\bar{p}$-space 3-D data manifold of Fig. 2 permitting thereby optical image retrieval of the 3-D object in slices parallel to the projection plane one at a time. For example, Fig. 1-b shows the projection hologram for the $\bar{p}$-space data obtained in a computer simulation of the arrangement shown in Fig. 1-a. The central cross-sectional outline of the object (the two 1 m diameter reflecting spheres of Fig. 1-a) retrieved from this projection hologram by means of a 2-D Fourier transform carried out on the optical bench is shown in Fig. 1-c. A similar example is shown in Figs. 3 and 4. Figure 3 shows a second test object consisting of 3-D distribution of a set of 8 point scatterers with locations and spacings given in the Figure. Figure 4 shows the projection holograms corresponding to the three slices of the object containing the point scatterers and the image retrieved from each. The sweep width in this example, as in the previous example, was (2-4) GHz however the number of receivers in the recording array has been reduced from 50 to 16. These computer simulations demonstrate that a 3-D (lateral and longitudinal) resolution of the order of twenty centimeters*is easily achieved with a frequency sweep covering only (2-4) GHz using a broad-band array of 16 receivers and one transmitter. Wider-spectral windows should yield better resolution. It is worthwhile to note in this respect that commercial microwave sweepers and synthesizers are available with a spectral coverage of (.1-25) GHz indicating a potential for practical resolutions of the order of possibility few centimeters with cost-effective broad-band apertures consisting of tens of receivers operating with one central illuminator.

(e) The viewing or the display of a true 3-D image of the various slices or cross-sectional outlines should be possible by reconstruction of the various projection holograms in rapid succession while projecting the reconstructed real images of the corresponding slices on a rapidly moving projection screen. The screen would be displaced rapidly (together with the Fourier transforming lens) on the optical bench in the axial directions by small amounts proportional to the distances between the various slices. In another approach we have found that the 2-D *virtual Fourier transform* of a projection hologram can be carried out by simply viewing (with the unaided eye) a transparency containing an array of reduced replicas of the projection hologram arranged side-by-side with a point source. The image retrieved in this fashion would lie in the plane of the point source. This approach has the potential for 3-D display by viewing the virtual images retrieved from a series of projection holograms corresponding to different slices or cross-sectional outlines

*This means 10^3 distinguishable 3-D resolution cells in the $(2 \times 2 \times 2)m^3$ volume of the assumed object.

of the object passed in front of the eye in rapid succession while moving the reconstruction point source axially back and forth at a suitable rate of incremental axial displacements. A proposed electro-optical scheme that permits carrying out this procedure in real-time using a rapidly recyclable spatial light modulator (SLM) operating in a reflection mode is shown in Fig. 5. The computer, the high resolution CRT and the projection optics are used to project reduced noncoherent images of the various projection holograms in rapid succession on the SLM while the axial position of the reconstruction point sources is altered rapidly also under computer control. The point source need not be derived from a laser in order to yield an image but could also be a miniature "grain of wheat" light bulb.

(f) As seen in (e), unlike monochromatic longwave holographic imaging, there is no specific scaling requirements imposed on the projection holograms in order to avoid longitudinal distortion in the optical reconstruction circumventing thus the wavelength scaling problem.

(g) Because of the broad spectral extent of the illumination used and ability to display the reconstructed image in separate slices, speckle or coherent noise, which is known to plague coherent imaging systems, is suppressed making the system behave in as far as image noise is concerned like a noncoherent imaging system but at the same time enjoy the superior detection characteristics associated with synchroneous detection techniques.

(h) The broad-band nature of the imaging process also helps suppress undesirable image detail that could arise from object resonances which could seriously degrade image quality in a monochromatic imaging system.

(i) The data collected at every receiver, represents after correction, essentially the frequency response of the scattering object measured from a different aspect angle. Assuming the scattering process is linear, this frequency response is related to the impulse response of the object by a Fourier transform (see ref. 5 in List of publications). This suggests that impulse illumination can be utilized instead of freguency swept illumination. When this is done,the 3-D data manifold in p-space may be generated by Fourier transforming the impulse response at each receiver, correcting the data for the Factor F mentioned in (b), and storing the result in the appropriate $\bar{p}$-space locations for each receiver. The resulting $\bar{p}$-space volume accessed in this fashion can then be employed as described earlier to yield 3-D image information. Impulse illumination is desirable in certain instances of rapid target motion but may be more difficult to implement than frequency swept illumination. Since the impulse reponse of a time invariant linear system can also be deduced from white noise excitation and corellation of the output response with the input as described elsewhere in more detail (see 5 in list of publications), it follows that the techniques described in this report for coherent broadband radiation should be equally applicable with minor signal processing modification to noise-like broadband

radiation including passive black-body radiation.

(j) Experimental verification for both the principle of frequency diversity imaging and the TDR concept were obtained with the aid of an available semi-automated network analyzer installed in a recently refurbished anechoic chamber with other funding (see Figs. 6 and 7). This versatile system is capable of vector (amplitude and phase) measurements of wavefields scattered from test objects situated in the anechoic chamber over any frequency range lying in the (.1-18)GHz range for a variety of polarizations. A test object consisting of two parallel cylinders 25 cm apart each 5 cm in diameter and 50 cm long was mounted on a rotating styrofoam pedestal that is under computer control and illuminated as shown in Fig. 8. The distance from the center of the object to the illuminating parabolic antenna to the left and the receiving horn feeding the network analyzer was 2.5 m. The complex frequency response of this object was measured in the (5-14)GHz range and the data stored for 128 object orientation covering 360°. The stored data was corrected for range-phase with a synthetic TDR generated in the computer and the corrected data displayed and photographed yielding the frequency swept hologram shown in Fig. 9 (c). The image retrieved from this hologram via an optical Fourier transform carried out on the optical bench is shown in Fig. 9 (d). For reasons of comparison a computer simulation of this experiment assuring a (2-18)GHz sweep was performed. The resultant range-phase corrected hologram and the image retrieved from it optically are shown in Fig. 9 (a) and (b). These results which should be viewed as preliminary (since measurement system errors have not been completely tracked down and neutralized) demonstrate conclusively the practical viability of frequency diversity imaging.

3. Conclusions.

The primarily analytical and numerical study of frequency diversity imaging performed under this grant demonstrates conclusively the feasibility of a new generation of coherent broadband imaging radars capable of furnishing 3-D image detail of distant target with cost effective giant apertures and efficient digital/optical signal processing.

Future work in this area will focus more on the analysis and identification of optimal methods for data acquisition, processing and 3-D display. The ultimate aim is the generation of design criteria for a prototype system and its assessment in the 3-D imaging of low flying aircraft passing within range of our facilities on route for landing at the Philadelphia Airport.

List of Publications

1. N.H. Farhat, "Frequency Synthesized Imaging Apertures", Proc. 1976, International Optical Computing Conference, IEEE Cat. #76 CH 1100-7C, pp. 19-24.

2. N.H. Farhat, M.S. Chang, J.D. Blackwell and C.K. Chan, "Frequency Swept Imaging of a Strip", Proc. 1976, Ultrasonics Symposium, IEEE Cat. #76 CH 1120-5SU.

3. J.D. Blackwell and N.H. Farhat, "Image Enhancement in Longwave Holography by Electronic Differentiation", Optics Communications, Vol. 20, Jan. 1977, pp. 76-80.

4. C.K. Chan, N.H. Farhat, M.S. Chang and J.D. Blackwell, "New Results in Computer Simulated Frequency Swept Imaging", Proc. IEEE (Letters), Vol. 65, pp. 1214-1215, Aug. 1977.

5. N.H. Farhat, "Principles of Broad-Band Coherent Imaging", J. Opt. Soc. Am., Vol. 67, pp. 1015-1020, Aug. 1977.

6. N.H. Farhat, "Comment on Computer Simulation of Frequency Swept Imaging", Proc. IEEE, Vol. 65, pp. 1223-1226, Aug. 1977.

7. N.H. Farhat, "Comment on a New Imaging Principle", Proc. IEEE (Letters), Vol. 66, pp. 609-700, May 1978.

8. N.H. Farhat, "Microwave Holographic Imaging - Prospects For a Real-Time Camera", SPIE, Vol. 180, *Real-Time Signal Processing II*, (1979).

9. N.H. Farhat and C.K. Chan, "Three-Dimensional Imaging by Wave-Vector Diversity", *Acoustical Imaging*, Vol. 8, A. Metherell (ed.), Plenum Press, New York (1980), pp. 499-515.

10. C.K. Chan and N.H. Farhat, "Frequency Swept Imaging of Three Dimensional Perfectly Reflecting Objects", IEEE Trans. on Antennas and Propagation - Special Issue on Inverse Scattering. (Accepted for publication.)

11. C.K. Chan, "Analytical and Numberical Studies of Frequency Swept Imaging", University of Pennsylvania, Ph.D. Dissertation (1978).

Related Publications

1. N.H. Farhat, "New Imaging Principle", Proc. IEEE (Letters), Vol. 64, pp. 379-380, March 1976.

2. N.H. Farhat, T. Dzekov and E. Ledet, "Computer Simulation of Frequency Swept Imaging", Proc. IEEE (Letters), Vol. 64, pp. 1453-1454, Jan. 1977.

3. G. Tricoles and N.H. Farhat, "Microwave Holography: Applications and Techniques", Invited paper, Proc. IEEE, Vol. 65, pp. 108-121, Jan. 1977.

4. M.A. Kujoory and N.H. Farhat, "Microwave Holographic Substraction for Imaging of Buried Objects", Proc. IEEE (Letters), Vol. 66, pp. 94-96, Jan. 1978.

5. M.A. Kujoory and N.H. Farhat, "Format Generation For Double Circular Scanners For Use in Longwave Holography", Acoustical Imaging and Holography, Vol. 1, No. 2, pp. 133-141 (1979).

6. N.H. Farhat and J. Bordogna, "An Electro-Optics and Microwave-Optics Program In Electrical Engineering", IEEE Trans. on Education - Special Issue on Optics Education (accepted for publication).

7. N.H. Farhat, "Holographically Steered Millimeter Wave Antennas", IEEE Trans. on Antennas and Propagation (accepted for publication).

List of Personnel

N.H. Farhat - Professor and Principle Investigator
M.S. Chang - Assistant Professor
J.D. Blackwell - Graduate Student and Research Fellow
C.K. Chan - Graduate Student and Research Fellow
C.Y. Ho - Graduate Student and Research Fellow

Degrees Awarded:

J.D. Blackwell - MSEE (1976)

C.K. Chan - Ph.D. (1978)

APPENDIX I

The Frequency Displaced Target Derived Reference

A second TDR method which we refer to as a *Frequency Displaced Target Derived Reference* (FDTDR) method also shows promise. This method involves simultaneous illumination of the object with two phase locked imaging frequencies ω_1 and $\omega_2 = \omega_1 + \Delta\omega$ that differ by a small frequency increment $\Delta\omega$. Referring to eq. (9) of ref. 10 (see list of publications) we can write for the far field at a given receiver location R_R,

$$\psi_1(k_1,R_R) = \frac{jk_1}{2\pi R_R} e^{-jk_1(R_T+R_R)} \int U(\bar{r})\, e^{-j\,\bar{p}_1\cdot\bar{r}}\, d\bar{r} \quad (1)$$

$$\psi_2(k_2,R_R) = \frac{j(k_1+\Delta k)}{2\pi R_R} e^{-jk_1(R_T+R_R)} e^{-j\Delta k(R_T+R_R)} \times \int U(\bar{r}) e^{-j\bar{p}_1\left(1+\frac{\Delta\omega}{\omega 1}\right)\cdot\bar{r}} d\bar{r} \quad (2)$$

where $k_{1,2} = \omega_{1,2}/c$ and $\Delta k = \Delta\omega/c$.

By making $\Delta\omega/\omega \ll 1$ the integral in (2) will approach that in (1). The only difference between the far fields ψ_1 and ψ_2 at the receivers is then the phase term $\Delta k(R_T + R_R)$. Measurement of this phase difference yields $(R_T + R_R)$ since Δk is known. This information can be used to correct the phase of either the ψ_1 or ψ_2 signals to obtain the required $\bar{p}$-space information.

$$\Gamma(\bar{p}) = \int U(\bar{r})\, e^{j\,\bar{p}\cdot\bar{r}}\, d\bar{r} \quad (3)$$

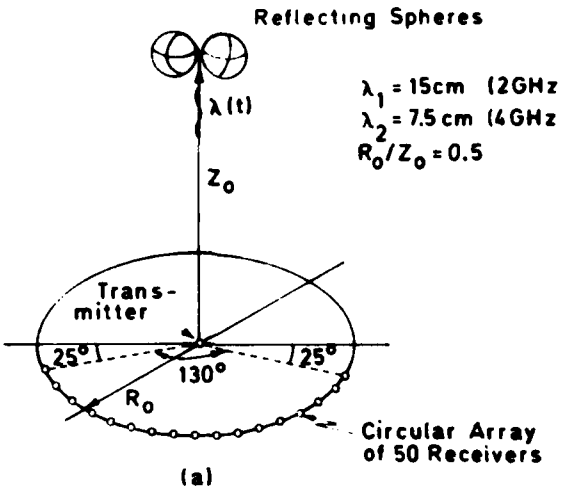

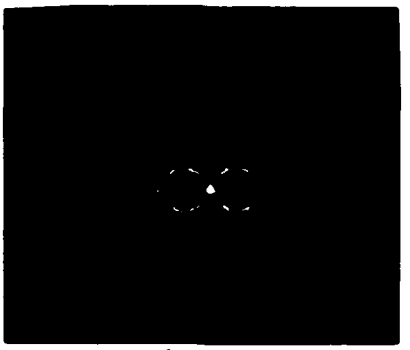

Fig. 1. Computer Simulation of Wave-vector Diversity Imaging, (a) Geometry, (b) Projection Hologram, (c) Retrieved Central Cross-sectional Image.

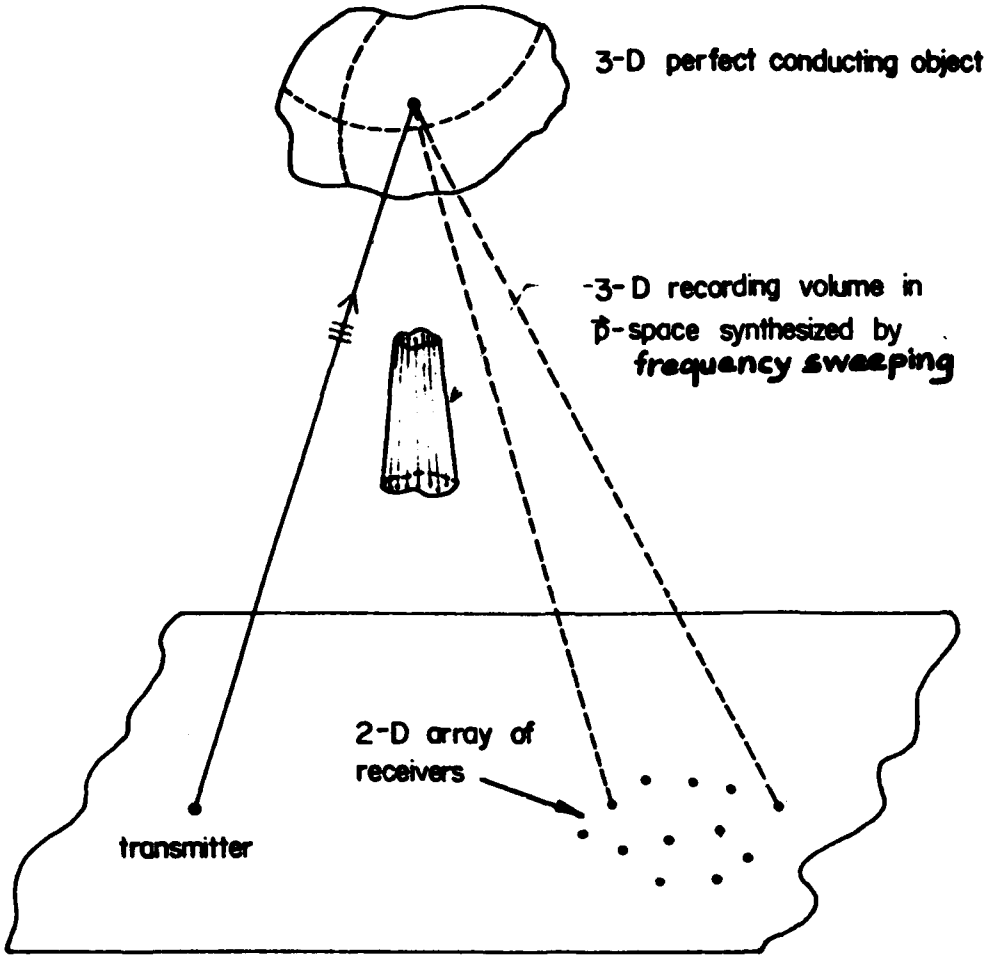

Fig.2 Three dimensional $\vec{p}$-space data generated by frequency sweeping and collected by a 2-D array of receivers.

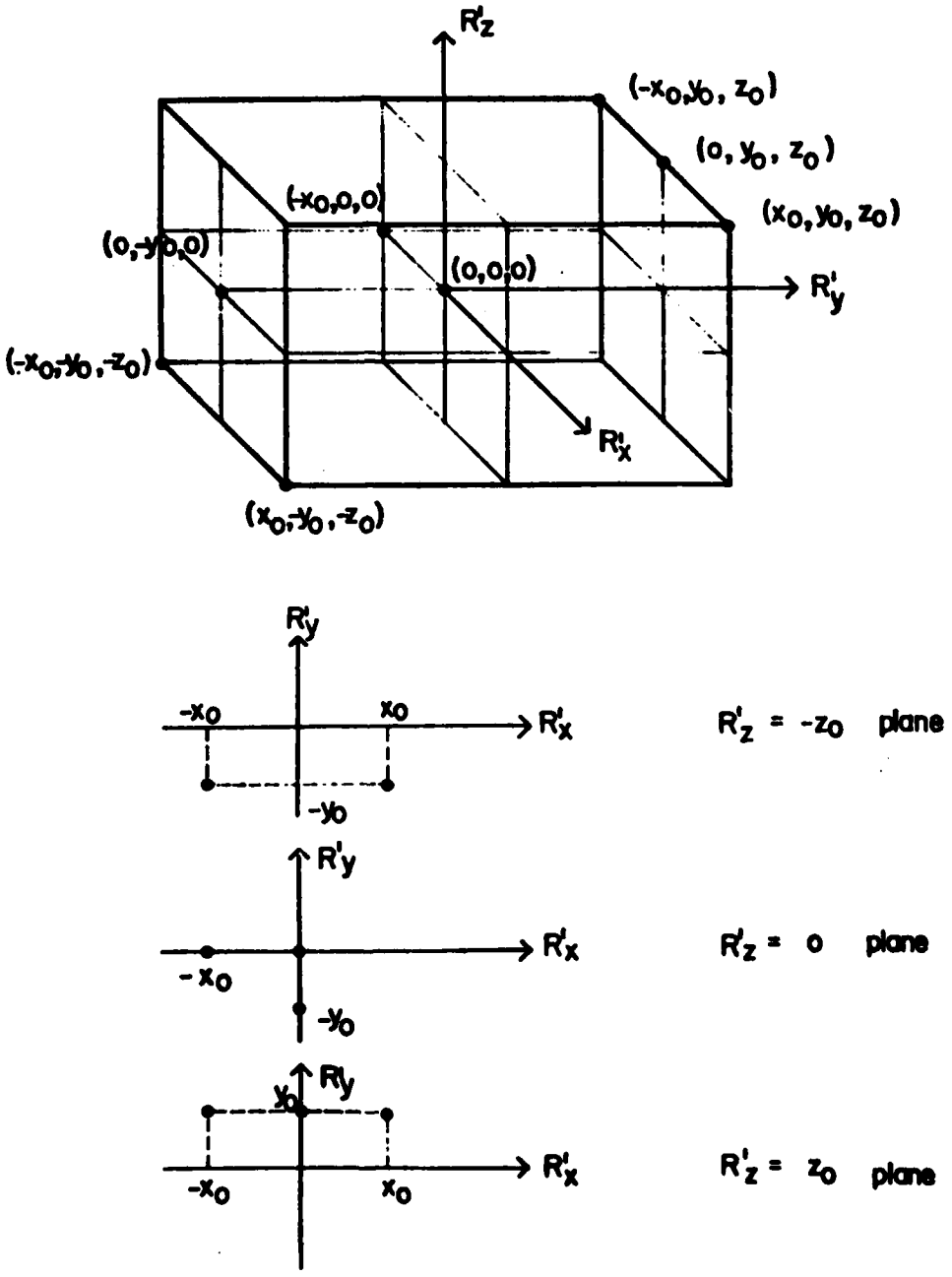

Fig. 3. 3-D object consisting of a set of eight point scatterers shown in isometric and R'_x-R'_y plane views at $R'_z=-z_o,0,z_o$. $x_o=y_o=z_o=100$ cm.

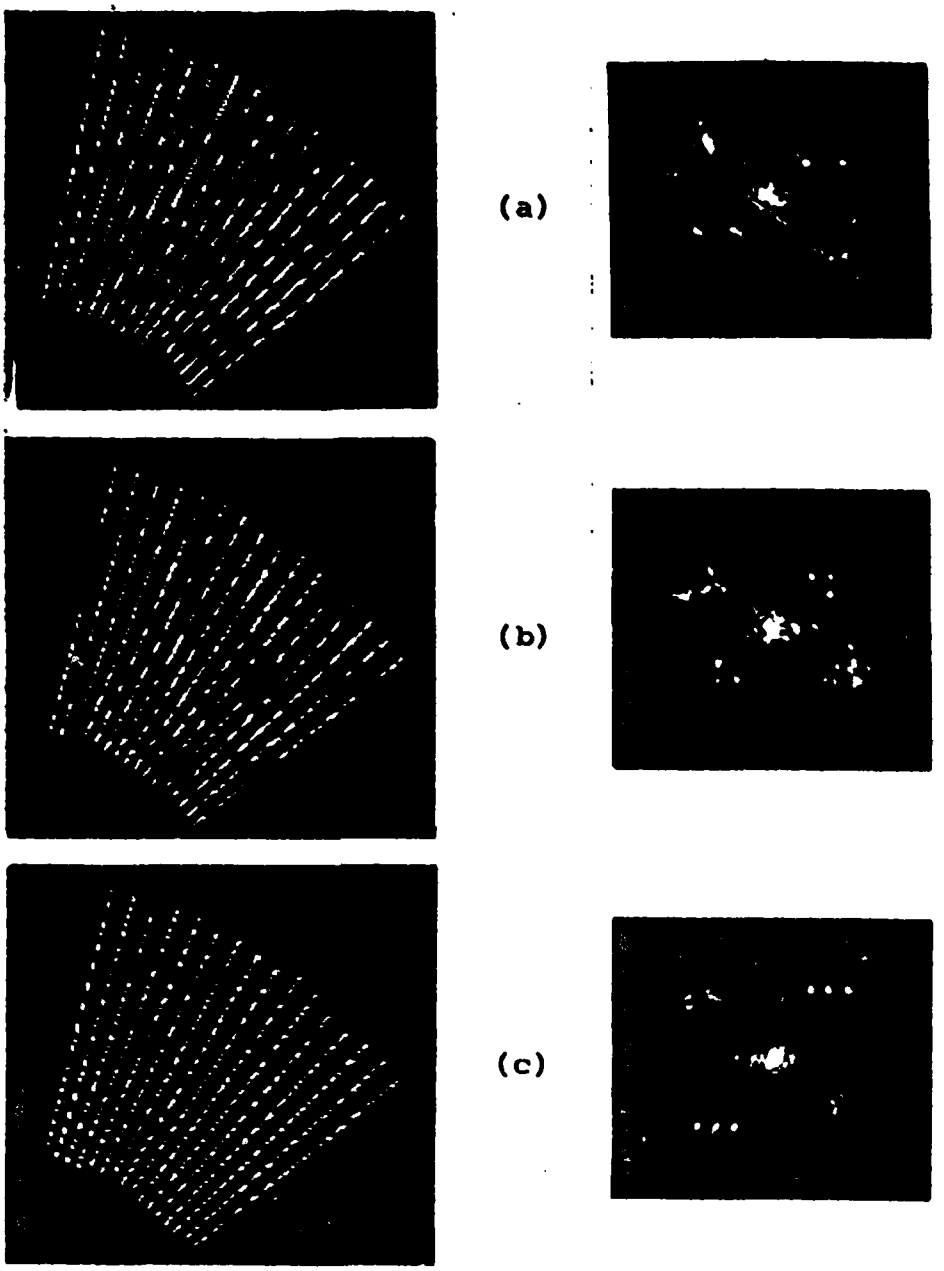

Fig. 4. Projection holograms and their optical reconstructions for the set of point scatterers in Fig.7.10 at different R'_z planes. (a) Hologram and reconstructed image of scatterers at $R'_z=-z_o$ plane. (b) Hologram and image at $R'_z=0$ plane. (c) Hologram and image at $R'_z=z_o$ plane. $x_o=y_o=z_o=100$cm.

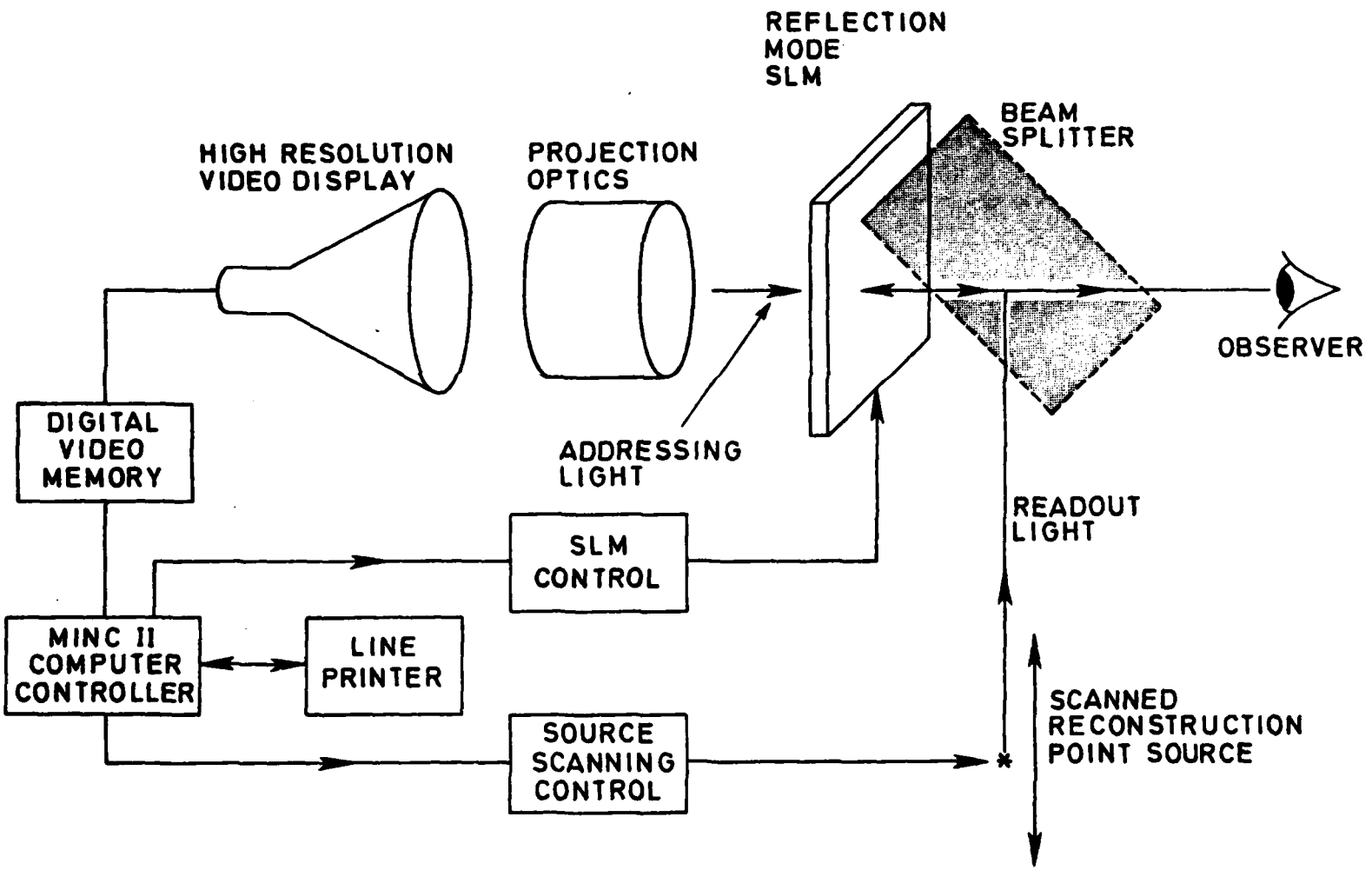

Fig. 5. True 3-D image reconstruction based on the virtual Fourier transform.

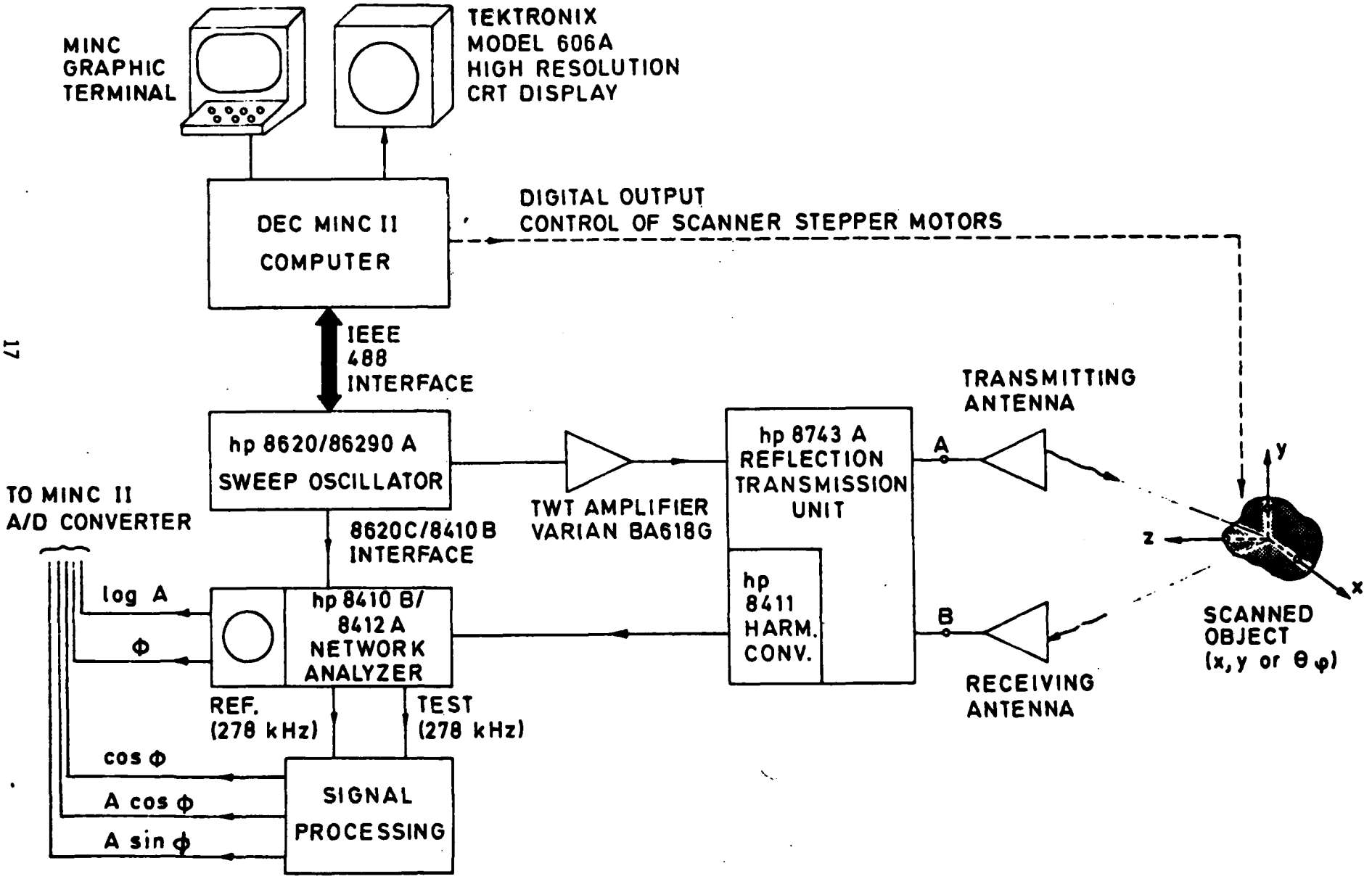

Fig. 6. Block Diagram of Automated Microwave Network Analyzer Showing Interface to MINC II Computer via IEEE 488 Standard Interface Bus.

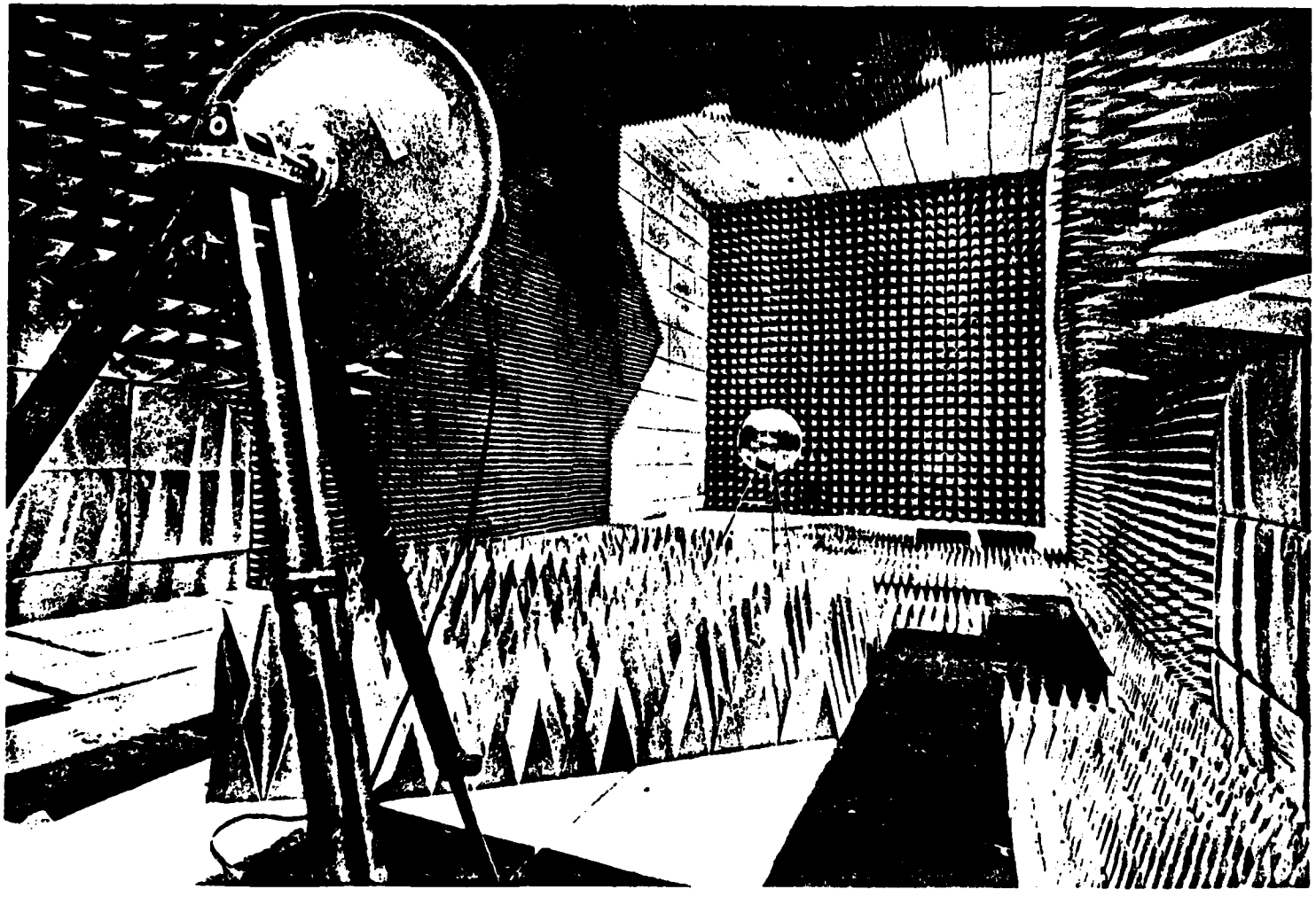

Fig.7. View of Microwave Anechoic chamber showing illuminator antenna and a calibration sphere in background.

(a)

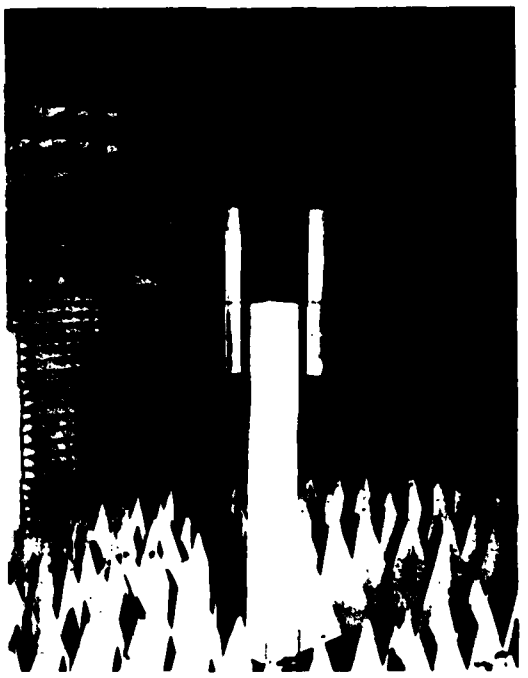

(b)

Fig. 8. Two views of dual-cylinder test object in Anechoic chamber. (a) View showing illuminator to the left and the receiving horn on the right separated by absorbing barrier. (b) View showing test object mounted on rotating styrofoam pedastel. Cylinders are 5 cm in diameter, 50 cm long, 25 cm apart.

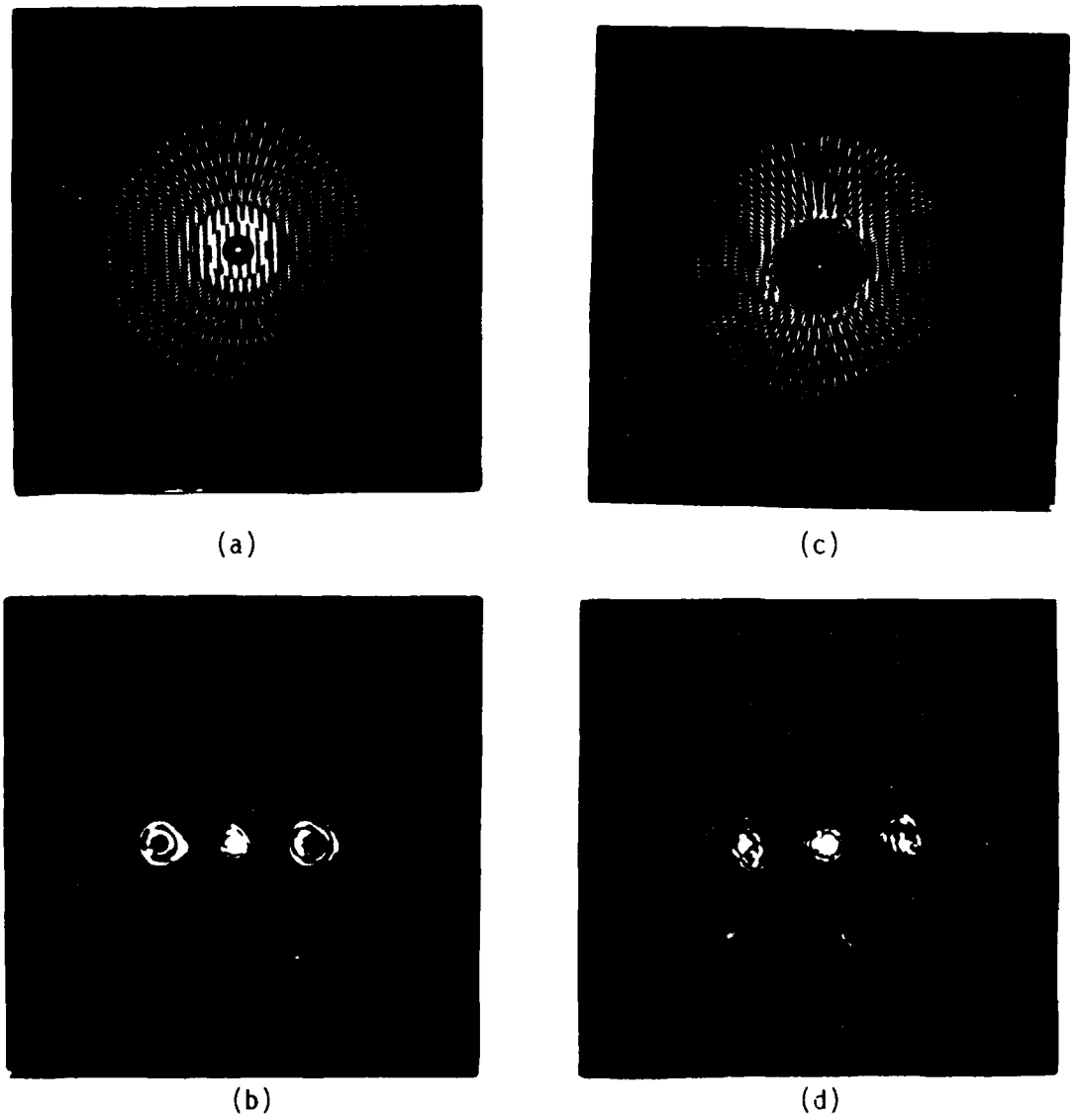

Fig. 9. Frequency swept holograms and retrieved images for a dual-cylinder test object. (a) Computed frequency swept hologram for a (2-18)GHz sweep and (b) retrieved image; (c) measured frequency swept hologram for a (5-14)GHz sweep and (d) retrieved image.